

## MICRO AXIAL HYDRAULIC TURBINE PROJECT WITH EMPHASIS ON RUNNER AND WICKET GATES PROFILES CALCULATION

Derli Dias do Amaral Junior [derli.amaral@usp.br](mailto:derli.amaral@usp.br)

Fabio Saltara [fsaltara@usp.br](mailto:fsaltara@usp.br)

Escola Politécnica da Universidade de São Paulo.

Av. Prof. Mello Morais, 2231 Cidade Universitária – SP - Brasil - CEP: 05508-030

[derli.amaral@usp.br](mailto:derli.amaral@usp.br), [fsaltara@usp.br](mailto:fsaltara@usp.br)

**Abstract.** The purpose of this work is to present a methodology to design a small axial hydraulic turbine with emphasis on the project of the profiles of the runner and wicket gate, including both analytical results and numerical results from a cascade panel method. Comparisons with field test measurements of a prototype are also presented. The analytical methodology used is the Wenig's inviscid flow theory which requires the evaluation of interference factors to model how lift and drag characteristics of the turbine cascade of blades are related to those of a single isolated airfoil. It is found that the Wenig's theory provides a reasonable prediction of the lift interference factor if both the angle of attack is relatively low and the thickness of the blades is relatively small when compared to the distance between the blades. The numerical methodology using the Hess and Smith's 2-D panel method for a cascade of blades and for an isolated airfoil was used in order to have a comparison with the analytical lift and drag. Prototype field test measurements of the turbine power output, in agreement with IEC-60041 standards, were carried out to evaluate the results using the analytical and numerical methods.

**Keywords:** Axial hydraulic turbine, cascade, panel method, field tests.

### 1. INTRODUCTION

The main objective of this work is to present a methodology used to design small axial turbine propellers, and present the field test measurements in order to evaluate if this methodology reaches the expected results. In this work we study a 20 kW hydraulic power plant, installed at *Fazenda Ipanema* in the city of Sorocaba, São Paulo, Brazil. This amount of delivered energy is characterized as a Micro Power Plant. This type of hydraulic plants falls in a range from 5 to 1 MW of energy production.

Micro power plants play an important role in remote locations. In Brazil regions like Amazon, where the lack of electricity power is often an obstacle to socio-economic development, energy from this kind of plants can be used for value-added primary production, generating jobs and revenues.

The idea is to compare an old analytical methodology to design sections of propellers blades to a modern numerical methods, in this case a panel method with emphasis in the lift coefficient. Lift Coefficient is the key variable to obtain the amount of power delivered from a propeller turbine.

Figure 1 shows the machine characteristics. This type of axial machine has permanent magnets located in the same plane of the runner blades, perpendicular to the flow direction. Due the fact that it has permanent magnets, excitation system is not required, thus in the moment that the machine spins 1 rpm it produces electrical voltage.

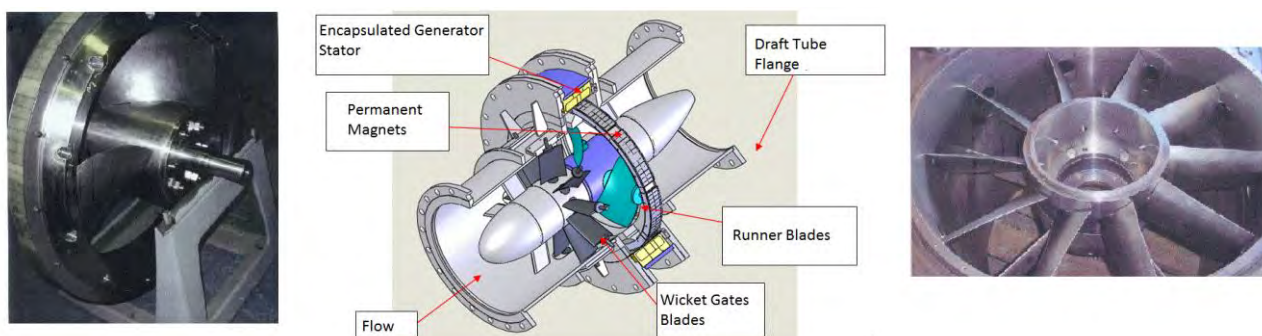


Figure 1. 20 kW Machine Characteristics; Left: Runner Blades with permanent magnets; Right: Wicket Gates (courtesy of Hydrel, June 5<sup>th</sup> 2013)

The hydraulic machine project is conceived to attend a specific water flow rate  $Q$  and gross head  $H_g$ . Those two parameters also indicate the most adequate type of hydraulic turbine to be selected. Table 1 shows the values used to calculate the machine. This design point is designated as the “rated point”.

Table 1.20 kW Machine Rated Point

Rated Turbine Power [kW]	20
Rated Efficiency [%]	70
Rated Flow [m <sup>3</sup> /s]	1.15
Net Head [m]	2.57
Rated Speed [rpm]	450
Rated Axial Thrust [kN]	45

## 2. PROPELLER SECTION CALCULATIONS (WICKET GATES AND RUNNER BLADES)

To define the propeller section we must define the profile zero lift angle, the profile curvature and the cascade profile ideal angle of attack.

### 2.1 NACA Series Choice

According to Kruppa (1969) the two most used sections used in propellers profiles are the NACA 16 and the NACA 66 sections. The advantage of these two profiles are low drag in high speed flow and good pressure distributions over the section.

The NACA 6-Series was derived using an improved theoretical method that, like the 1-Series, relied on specifying the desired pressure distribution and employed advanced mathematics to derive the required geometrical shape. The goal of this approach was to design airfoils that maximized the region over which the flow remains laminar (Breslin, 1961). The decision to use the NACA 66 section relies on these combined characteristics, however this is not enough to have the finally chosen profile.

A cambered airfoil is usually designed to increase the maximum lift while maintaining a smooth flow over the leading edge. According to Kruppa (1969) the two most used camber lines for propellers are the  $a=1.0$  and the  $a=0.8$  mean line. Where in the ideal flow the  $a=1.0$  mean line appears to offer the most favorable characteristics as far as maximum pressure drop is concerned, it requires large corrections in viscous flows. The corrections for the NACA  $a=0.8$  mean line are small, thus favoring its use for the design of blade propellers (Abbott, 1958). Figure 2 shows the properties of the NACA 66 modified line  $a=0.8$  geometry as function of the section maximum thickness  $t_0$  and maximum mean line ordinate  $f_0$ . Additionally, as an example, in the same figure, we have the transformation from the dimensionless geometry to a prototype geometry (Runner Blade Section at  $\chi=0.4$ ). Where  $\chi$  is the percentage of the Runner's diameter.

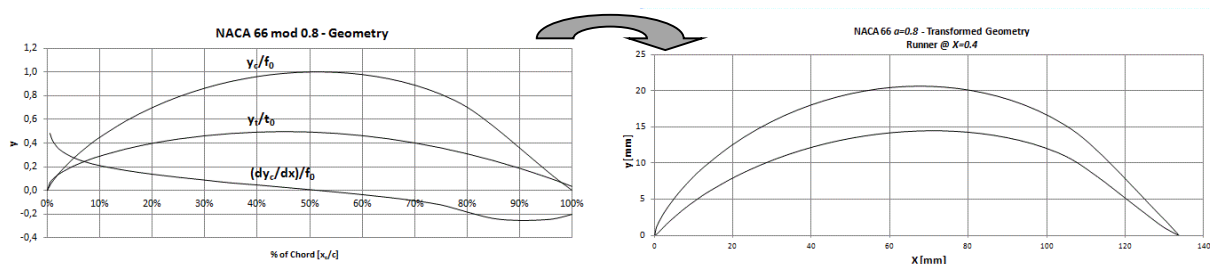


Figure 2. NACA 66 Serie with modified mean line –  $a=0.8$  (courtesy of Hydrel, April 1<sup>st</sup> 2013)

### 2.2 Propeller Section Definition

As stated before, to have the final prototype section we have to define the zero lift angle, the profile curvature and the cascade profile ideal angle of attack.

Figure 2 shows the reference surface trace that represents the flow passing through a row of cascade blades. According to Gostelow (1984), due to rotation and boundary layer formation, the flow in an actual turbo machine is three dimensional. Assuming the flow to be two dimensional makes our problem quite easy. To do so we neglect the blade height and delineate a plane  $ZY^*$  in a given radius  $r$  of the cylinder shown in Fig. 3b. In axial machines flow is assumed to be two dimensional.

The design point, which is where the section has to be positioned along of the  $ZY^*$  planes, is the condition of “shock free entry” and the tangential velocities at the runner exit at every section of the rotor is zero.

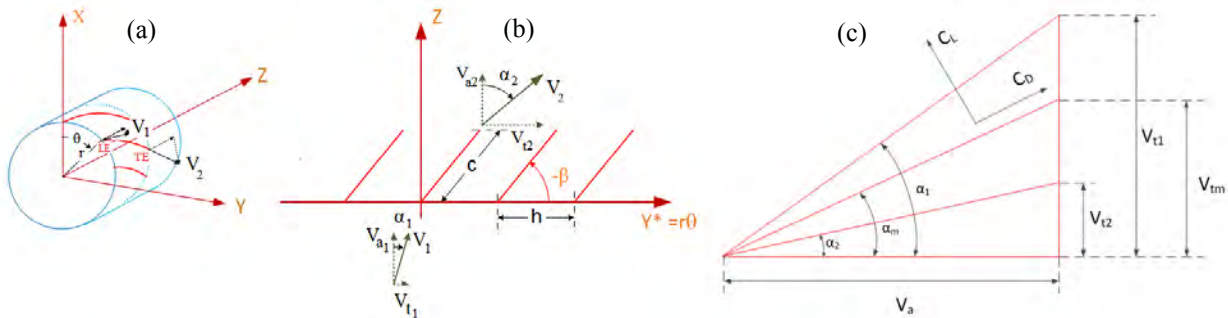


Figure 3. Reference Surface Trace; (a): XYZ plane; (b): ZY\* plane; (c): Scheme of notation for defining lift and drag coefficient in two-dimensional cascade.

The inclination angle  $\beta$  of the relative trace to the  $Y^*$  axis is the flat plate thin section zero lift angle. According to Twhaites (1987) the flow is a periodic repetition in  $h$  intervals measured parallel to  $Y^*$ . This periodicity implies that it is sufficient to consider a single interval with this space to establish the main characteristics of flow.

The circulation  $\Gamma$  around a profile can be calculated considering a consistence contour of two stream lines separated by a distance  $h$  and connected by lines parallel to the  $Y^*$  axis in big distances before and after the hydrofoil. The sum of two identical stream lines contributions is zero. Then, for the circulation:

$$\Gamma = (V_{t1} - V_{t2})h = V_a h [\tan(\alpha_1) - \tan(\alpha_2)] \quad (1)$$

The tangent velocity vectors  $V_{t1}$  and  $V_{t2}$  at the entry and exit are at water angles  $\alpha_1$  and  $\alpha_2$  respectively. The variable  $V_a$  is the axial entrance velocity.

The rise in static pressure across the turbine cascade is expressed in terms of the entry tangential velocity  $V_{t1}$ , the exit tangential velocity  $V_{t2}$  and the pressure loss  $\bar{p}$  which appears due the viscosity, is:

$$p_2 - p_1 = \frac{1}{2} \rho (V_{t1}^2 - V_{t2}^2) - \bar{p} \quad (2)$$

The lift coefficient (Twhaites, 1987) depends on the medium cascade flow angle  $\alpha_m$ , drag coefficient  $C_d$ , solidity ratio  $S_c$  and the gap chord ratio parameter  $k$ .

$$C_{Lo} = Abs \left[ \frac{4}{S_c k} \frac{\sin(\alpha_m + \beta)}{\cos(\beta)} \right] - C_d \tan(\alpha_m) \quad (3)$$

The Solidity Ratio is the ratio of the total rotor blade area, which is the combined area of all the main rotor blades, to the total rotor disc area and can be expressed by the ratio between chord  $c$  and the space between the chords  $h$  as given in the Eq. (4).

$$S = \frac{c}{h} = \left( \frac{Z}{2\pi\chi R} \right) c \quad (4)$$

We change the solidity ratio for the runner or wicket gates for our analyses introducing the number of blades  $Z$ , the dimensionless runner-hub radius ratio  $\chi$  and the runner diameter  $R$ .

In order to know the lift coefficient we have to determine the drag coefficient, and it is given by (Twhaites, 1987).

$$C_d = \sum_0^4 a_n \left( \frac{t_0}{c} \right)^n \quad (5)$$

The drag coefficient is related to the maximum chord-thickness ratio  $t_0/c$  and  $a_n$  which are the coefficients of a fourth-degree polynomial.

The parameter  $k$  included in Eq. 3 is given by Twhaites (1987) and determine the gap-chord ratio.

$$\frac{k+1}{k-1} = u = \frac{\tan(\alpha_1) + \tan(\beta)}{\tan(\alpha_2) + \tan(\beta)} \quad (6)$$

We can rearrange the Eq. 6 in terms of  $k$ :

$$k = \frac{2\tan(\beta) + \tan(\alpha_1) + \tan(\alpha_2)}{\tan(\alpha_1) - \tan(\alpha_2)} \quad (7)$$

Derli Dias do Amaral Junior, Fabio Saltara  
Micro Axial Hydraulic Turbine Project with Emphasis on Runner and Wicket Gates Profiles Calculations

The parameter  $m$  in the Eq.8 establishes a relation between the lift coefficient for a cascade of foils and the one for a given isolated foil.

$$m = \frac{C_{L0}}{C_{isol.}} = \left(\frac{2}{\pi}\right) \left(\frac{h}{ck}\right) \left(\frac{1}{\cos(\beta)}\right) - \left(\frac{C_d}{2\pi}\right) \frac{\tan(\alpha_m)}{\text{abs}[\sin(\alpha_m + \beta)]} \quad (8)$$

The variation of the zero lift angle and gap-chord ratio of the characteristics of cascades of foils is illustrated in Fig. 4. This is an important graphic which says that as we increase the gap  $h$  between the foils the relation  $m$  tends to unity. It means that the cascade lift coefficient tend to be the isolated lift coefficient.

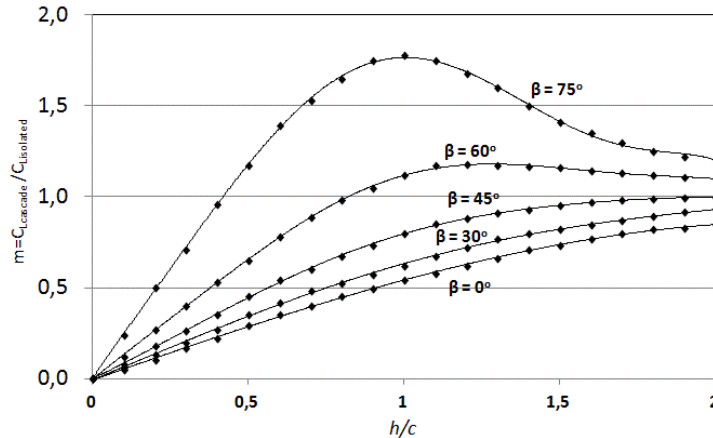


Figure 4. The effect of zero lift angle and gap-chord ratio on the lift of a cascade. From Twhaites (1987).

Twhaites (1987) gives us a relation to determine  $\beta$ , the zero lift angle for a flat plate foil, from the chord-gap ratio  $c/h$ , entrance and exit angle  $\alpha_1$  and  $\alpha_2$  respectively:

$$F \equiv 0 = \pi \frac{c}{h} - \ln(u) \cos(\beta) - 2\theta \sin(\beta) \quad (9)$$

Where:

$$\theta = \tan^{-1} \left( \frac{\tan(\beta)}{k} \right) \quad (10)$$

The Eq. 9 is solved numerically to determine the zero lift angle  $\beta$  using the entrance angle  $\alpha_1$ , exit angle  $\alpha_2$ , Eq. 7 and Eq. 10.

The first estimative of  $\beta$  is  $\beta_{est1} = f\alpha_2$  with  $f > 1.0$ . The angle  $\beta$  determined by the Eq. 9 is the angle  $\beta_{zl}$  from which the profile is positioned to develop the required lift. At each dimensionless ratio  $\chi$ , the profile should be positioned in relation to the mean flow, defined by the angle  $\alpha_m$ .

In this way we can define how the blade will be twisted in order to deliver the enough lift required by the machine on each section.

## 2.2 Cavitation on Propeller Blades (Wicket Gate and Runner)

In order to decide whether or not a particular foil section might be suitable to serve as a basis for designing propeller blade sections one has to know its pressure distribution over a sufficiently wide range of angles of attack. So the designer has to look at the value of minimum pressure somewhere on the foil surface. If the minimum pressure drops below a certain critical pressure of the fluid, cavitation may occur.

According to Kruppa (1969), given a local cavitation number  $\sigma_x$  and a safety cavitation onset  $S$ , if the maximum permissible pressure drop is known for each blade section and if the strength calculation requires a minimum blade section thickness, the maximum permissible thickness-chord ratio  $t_0/c$  can be calculated using Eq. 11:

$$\left(\frac{t_0}{c}\right)_{cav} = \frac{\left[\left(\sqrt{\frac{1+\sigma_x}{1+S_{cav}}}-1\right)-C_{2,cL}\right]}{c_1} \quad (11)$$

The constant  $C_1$  measures the profile section quality in relation to the displacement effect and its value depends on the NACA profile, where  $C_1 = 1.28$  for NACA 66. The constant  $C_2$  measures the quality of a mean line and depends on how cambered the section is, mean lines with  $a = 0.8$  receives  $C_2 = 0.278$ .

Differently from ship propellers where the cavitation number depends on how drowned the propeller is, turbine cavitation number depends on the stagnation pressure related to the section's relative velocity  $V_{tm}$ :

$$\sigma_x = \frac{2 \cdot (p_{0epx} - p_v)}{\rho (k_{wm} \cdot V_{tm})^2} \quad (12)$$

The term  $k_{wm}$  is used in order to correct the tangential velocity  $V_{tm}$  due to the profile thickness distribution. The cavitation number also depends on the water density  $\rho$ , the vapor pressure  $p_v$  and the pressure that is taken just before the blade section's flow entrance  $p_{0epx}$ .

For each section of the blade, from  $\chi = \frac{r}{R_R} = \min$  to  $\chi = 1$ , the relation  $(t_0/c)_{cav}$  is compared to the structural thickness-chord  $(t_0/c)_{st}$  ratio in order to avoid the cavitation inception. If the cavitation limit for one of the sections is lower than the structural thickness-chord limit  $(t_0/c)_{cav} < t_0/c$ , cavitation may occur and the turbine project has to be reviewed. In this case probably the hub-runner diameter ratio  $R_b/R_R$  will be higher than it was supposed to be and consequently the tangential velocity  $V_{tm}$  will be changed.

### 3. PANEL METHOD

As exposed in the introduction, the idea is to compare an analytical methodology to design sections of propellers blades to a numerical method. The panel method in this case is used to compare the wicket gate and runner sections lift coefficients. To do so every section is positioned at the same incidence angle obtained from the analytical calculation.

There are many choices to formulate a panel method. The simplest and truly practical one is given by Hess and Smith (LEWIS, 1991) and it is based on a distribution of sources and vortices on the surface of the geometry. In their method:

$$\phi = \phi_\infty + \phi_S + \phi_V \quad (13)$$

Where  $\phi$  is the total potential function and its three components are the potentials corresponding to the free stream  $\phi_\infty$ , the source distribution  $\phi_S$ , and the vortex distribution  $\phi_V$ . These last two distributions have locally varying strengths  $q_S$  and  $\gamma_S$ , where  $S$  is an arc-length coordinate which spans the complete surface of the airfoil in any way you want.

The potentials created by the distribution of sources/sinks  $\phi_S$  and vortices  $\phi_V$  are given by:

$$\phi_S = \int \frac{q(S)}{2\pi} \ln r \, ds \quad (14)$$

$$\phi_V = - \int \frac{\gamma(S)}{2\pi} \theta \, ds \quad (15)$$

Where the various quantities are defined in the Fig. 5:

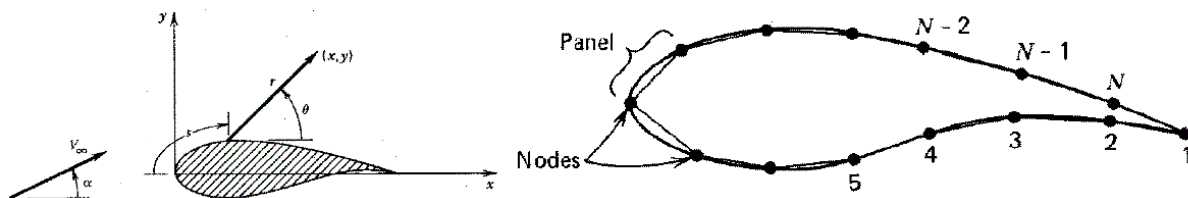


Figure 5. Panel Method quantities on the right side: Nodes and Panels and on the left side the quantities presented in the Eqs. 13 and 14. From Lewis (1991).

Notice that in these formulas, the integration has to be carried out along the complete surface of the airfoil. Using the superposition principle, any such distribution of sources/sinks and vortices satisfies Laplace's equation, but it is necessary to find conditions for  $q_S$  and  $\gamma_S$ , such that the tangential flow boundary condition and the Kutta condition are satisfied.

The Kutta condition encapsulates the observation that the flow cannot go around the trailing edge, but must leave the airfoil there. This is a consequence of viscous effects, which are otherwise absent from the calculation. For the Kutta condition to be satisfied the strengths of the vortex panels must be equal and opposite where they meet at the trailing-

edge joint (LEWIS, 1991). All that now remains is the solution of  $N+1$  simultaneous equations for the  $N+1$  unknown strengths (via a matrix inversion), and then the evaluation of the flow properties of interest. This is precisely what is done by the Vortex Panel Method.

We can have Eq. 13 in a discrete way shown in the Eq. 16:

$$\phi = V_\infty(x \cos \alpha + y \sin \alpha) + \sum_{j=1}^N \int \left[ \frac{q(s)}{2\pi} \ln r - \frac{\gamma(s)}{2\pi} \theta \right] ds \quad (16)$$

Since Eq. 16 involves integrations over each discrete panel on the surface of the airfoil, we must somehow parameterize the variation of source and vortex strength within each of the panels. Since the vortex strength was considered to be a constant, we only need to worry about the source strength distribution within each panel.

This is the major approximation of the panel method. However, you can see how the importance of this approximation should decrease as the number of panels  $N \rightarrow \infty$  and of course this will increase the cost of the computation considerably, so there are more efficient alternatives. Hess and Smith decided to take the simplest possible approximation, that is, to take the source strength to be constant on each of the panels.

$$q(s) = q_i \text{ on panel } i, \quad i = 1, \dots, N \quad (17)$$

Therefore, we have  $N + 1$  variables to solve in our problem: the  $N_i$  panel source strengths  $q_i$  and the constant vortex strength  $\gamma$ . Consequently, we will need  $N + 1$  independent equations which can be obtained by formulating the flow tangency boundary condition at each of the  $N$  panels, and by enforcing the Kutta condition discussed previously. The solution of the problem will require the inversion of a matrix of size  $(N + 1) \times (N + 1)$ .

The final question that remains is: where should we impose the flow tangency boundary condition? Hess and Smith choose to locate the control points at the midpoint of each of the panels. Although this method suffers from a slight alteration of the surface geometry, it is easier to implement and yields fairly accurate results for a reasonable number of panels. This location is also used to impose the Kutta condition (on the last panels on upper and lower surfaces of the airfoil, assuming that their midpoints remain at equal distances from the trailing edge as the number of panels is increased).

The implementation of the panel method code was developed in this study using the MATLAB program. The code used was formulated by Lewis (1991) to perform a panel method for an isolated foil section. Using the code we can visualize the pressure coefficient distribution  $C_p$  as function of the chord  $c$ , the lift coefficient  $C_L$  versus the angle of attack  $\alpha$  and the vector distribution plot around the section.

Figure 6 shows the MATLAB panel method results for a wicket gate section at  $\chi=0.39$ .

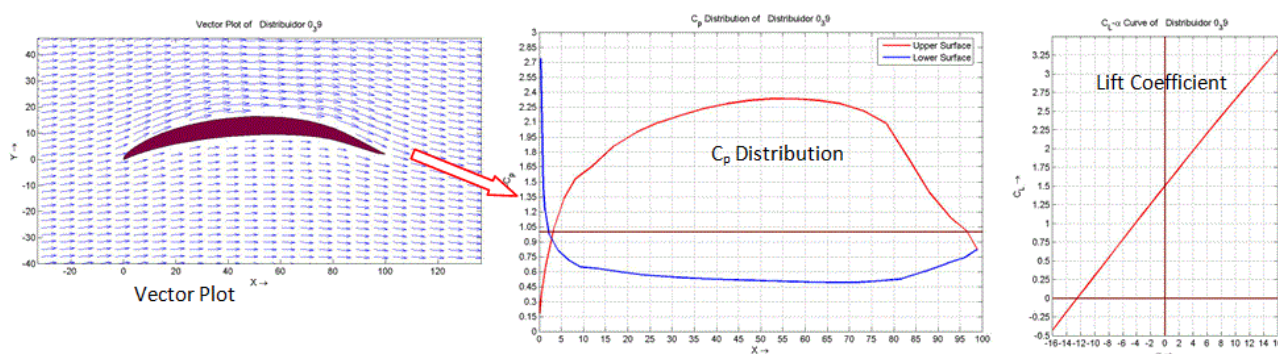


Figure 6. Panel Method results.

#### 4. TURBINE POWER CALCULATIONS

The propeller power calculation depends on the overall torque developed by the turbine runner  $T_t$ , minus the torque developed due the hydrodynamic loss in the water gap  $T_{ta}$  between the permanent magnets and the generator stator and the turbine angular speed  $\omega$  as shows the Eq. 18.

$$P_t = |T_t + T_{ta}| \cdot \omega \quad (18)$$

As the hydrodynamic loss torque  $T_{ta}$  is very small it can be neglected from Eq. 17. The turbine power is calculated in just one blade and then multiplied by the number of blades. The torque  $T_t$ , according to Kruppa (1969), depends on the number of blades  $Z$  and the torque per unit blade  $T_t/Z$  as shown in the Eq. 19.

$$M_t = \left(\frac{T_t}{Z}\right) \cdot Z \quad (19)$$

The torque per unit blade, Eq. 20 depends mainly on the torque coefficient  $C_T$ , which sums up the contributions of all sections of the blade, and it depends on the axial velocity  $V_a$  (see Fig. 3) and the runner radius  $R_R$  as well.

$$\frac{T_t}{Z} = C_T \cdot 0,5 \cdot \rho \cdot (V_a \cdot R_R)^2 \cdot R_R \quad (20)$$

In order to integrate all contributions, the blade is divided in a finite equally spaced number of sections counting from the hub to the runner diameter. The parameter  $D_x$  defines the percentage gap between two sections and depends on the number of the blade sections, which are in this case 12 and the hub diameter  $\chi_b$ .

$$D_x = \frac{1-\chi_b}{12} \quad (21)$$

With this we can sum the torque coefficient from every section as shown in the Eq. 22.

$$C_T = \frac{D_x}{Z} \cdot \int_{\chi_b}^{\chi_R} \frac{dC_{Ti}}{d\chi} d\chi \quad (22)$$

Every increment of each torque coefficient is given by the tangential force coefficient  $C_{Fti}$  on every section of the propeller times the dimensionless radius  $\chi$ .

$$\frac{dC_{Ti}}{d\chi} = \frac{dC_{Fti}}{d\chi} \cdot \chi \quad (23)$$

Finally we can visualize the contribution of the lift coefficient  $C_{Lx}$  for the calculation of the required power. The tangential force coefficient  $C_{Fti}$  also depends on the section runner tangential velocity  $W_m$ , the chord-radius ratio  $c/R$ , the medium cascade flow angle  $\alpha_m$  and the drag-lift ratio  $\varepsilon$ .

$$\frac{dC_{Fti}}{d\chi} = \left(\frac{W_m}{V_a}\right)^2 \cdot \frac{c}{R} \cdot C_{Lx} \cdot [\cos(\alpha_m) - \varepsilon \cdot \sin(\alpha_m)] \quad (24)$$

This is the procedure used to calculate the machine power.

## 5. FIELD TEST MEASUREMENTS

The main objective of a turbine field measurement is to check the turbine efficiency  $\eta_t$  comparing it to model test efficiency, or in the case of this study, compare it to the project efficiency. The procedure to prepare and run the test is given by IEC 60041 (1991).

The hydraulic turbine efficiency is given by the Eq. 25, and depends of the turbine power  $P_t$ , water flow  $Q$  and the net head  $H_n$ .

$$\eta_t = \frac{P_t}{\rho g Q H_n} \quad (25)$$

Basically the net head  $H_n$  is the net hydraulic energy that the machine uses to produce power. The difference between the head water level and the tail water level gives the gross head  $H_g$ , however there are energy losses to be discounted to obtain the turbine power.

The Eq. 26 given by (IEC 60041, 1991) shows the net head formula which depends on the pressure and velocity difference between the turbine inlet, point 1, and the draft tube outlet, point 2 (see Fig. 7) and the physical distance between the two measuring points  $Z$ .

$$H_n = H_g - \Delta P = \frac{p_1 - p_2}{\rho g} + \frac{v_1^2 - v_2^2}{2g} + Z \quad (26)$$

The most difficult variable to measure and control in a hydraulic turbine test is the water flow  $Q$ . There are various methods described by IEC 60041 (1991). As we are dealing with a micro power plant and one of the project objectives is minimizing costs, the chosen method was the sharp-crested rectangular weir, which is an overflow structure, built across open channels to measure the volumetric rate or water flow. Figure 7 (right) shows the overflow structure and

Eq. 27 gives the relation to calculate the water flow. The flow  $Q$  depends on the rectangular width  $b$ , on the height  $h$ , gravity acceleration  $g$  and on a constant  $\mu$ .

$$Q = \frac{2}{3} \mu \cdot b \cdot h^{3/2} \cdot \sqrt{2 \cdot g} \tag{27}$$

Normally in hydro turbine tests it is not possible to choose the desired net head. The customer and the manufacturer schedule a day to run the tests and the net head has to stay in between an operation range of heads. In the day of the test the several power operating points are measured and the most important point to be focused on is the rated point, if possible. This point gives the best efficiency for that specific head. After the test the prototype efficiency curve can be compared with the project or the model test curve. During the test the power delivered from the turbine was used to heat water in a reservoir.



Figure 7. Turbine measuring points; (a): IEC 60091 turbine measuring points, (b): 20 kW Machine during the test (courtesy of Hydrel, May 8<sup>st</sup> 2013)

6. RESULTS

One of the results that have to be checked in this work is the comparison between the analytical methodology and the numerical data. Figure 8 shows the wicket gate and the runner lift coefficient comparison along the chord at the same dimensionless ratio  $\chi$ . As we reach the tip of the blades the lift coefficient is getting lower, the main reason for that is due the tangential velocity  $V_{tm}$  that increases towards the tip. Figure 8 shows a good agreement between the analytical methodology and the numerical panel method.

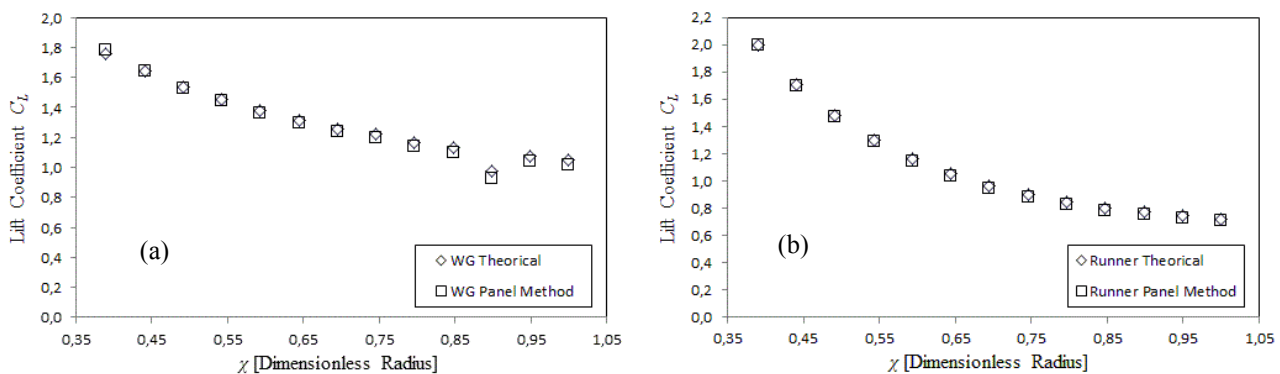


Figure 8. Lift coefficient comparison between theoretical versus Panel Methods; (a): Wicket Gate; (b): Runner

The other important comparison to be made is the project versus measured turbine efficiency  $\eta_t$ . As mentioned before, during the test water in a reservoir was heated by a set of resistance. The Fig. 9 shows two sets of measurements, the first one supplying a 20 kW resistance bank and the second 25 kW. On the left the Fig. 9 shows the power variation as the wicket gate changes its position for the two sets of bank resistance. On the right the Fig.9 shows the turbine efficiency for the same wicket gate points shown on the left side. Additionally the project rated efficiency point is placed in order to compare to the efficiency measurements. Error bars represents the test efficiency uncertainty. The results show that the project efficiency is in accordance to the measurement considering the error bar.

Due the draft tube discharge configuration, which is very close to the wall (See Fig. 7), and the water supply circuit the overall plant efficiency was affected i.e. the difference between the gross head  $H_b$  and the net head  $H_n$  in this case is higher than it's supposed to be in a standard configuration. But in the other hand this is a simple and economic configuration that compensates the efficiency loss if you have in mind that we are dealing with micro power plants.

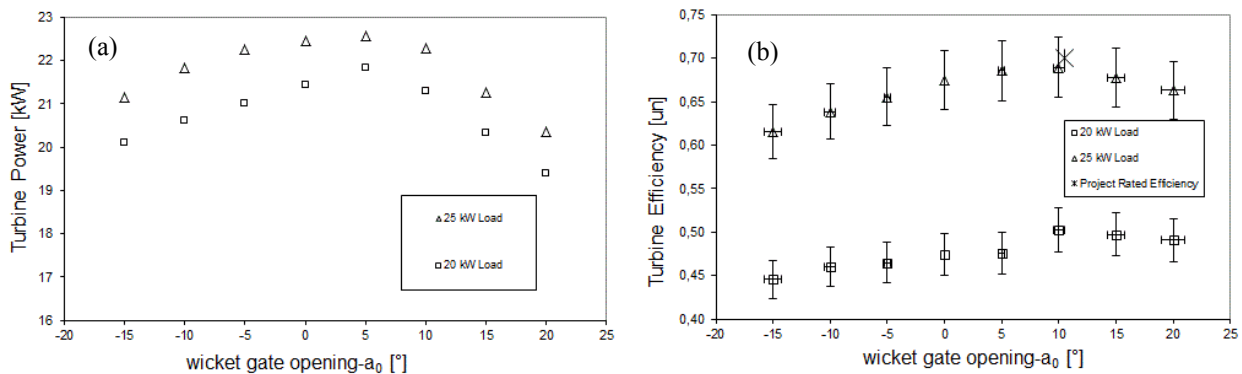


Figure 9. Field test measurements results. (a): Turbine Power; (b): Turbine Efficiency.

In order to see some of the analytical results Fig. 10 shows some of the blades and machine dimensions. In total the machine have three runner blades and ten wicket gates blades made of ASTM 304 Stainless Steel. As we can see in the Fig. 10 the wicket blades have a constant maximum thickness  $t_0$  and a constant chord length  $c$ , the reason for that is the cost to cast the blades.

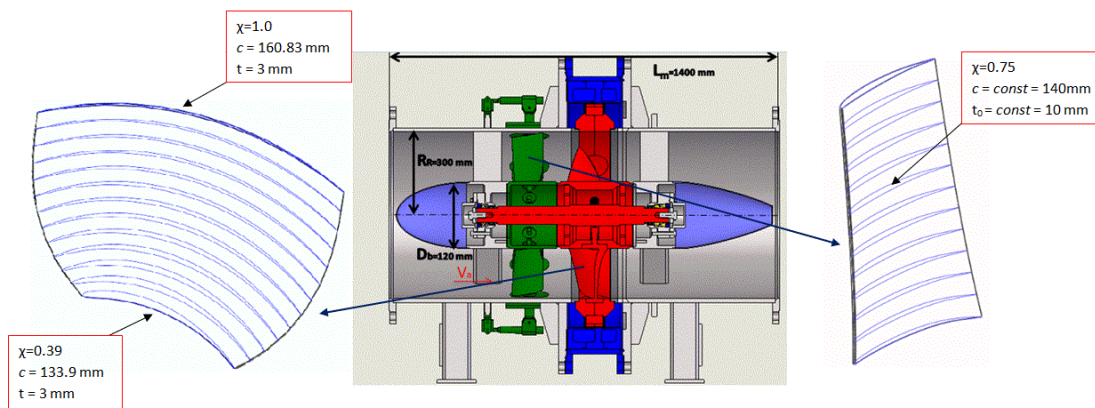


Figure 10. 20 kW Machine Properties; Left: Runner Blades; Right: Wicket Gates. (courtesy of Hydrel, May 26<sup>st</sup> 2013)

## 7. CONCLUSIONS

An outline of an analytical method for the runner and wicket gate profiles for an axial turbine has been presented. Suitable section performance analysis, which also include cavitation criteria, are required for the detailed design of the turbine blades.

In order to verify the analytical method presented, a two-dimensional vorticity panel method performed shows a good agreement with the blades lift coefficient curves, which is the most important factor to determine the unit rated power.

Field test measurements took place in order to compare the project and the prototype turbine efficiency. Fig. 9b shows the comparison between the analytical and prototype efficiency point showing a good agreement if we consider the error bar interval.

Micro hydro power plants have normally a lower efficiency rated point if compared with regular hydro installation. However, micro hydro power plants can be a very good option for remote locations and for this reason; the turbine efficiency cannot be the most important factor to consider if compared to the total cost involved.

A recommendation for further study would be a Computational Fluid Dynamics analysis to verify the machine flow behavior introducing the viscous effect that the presented analytical method neglected.

Derli Dias do Amaral Junior, Fabio Saltara  
 Micro Axial Hydraulic Turbine Project with Emphasis on Runner and Wicked Gates Profiles Calculations

## 8. ACKNOWLEDGEMENTS

I would like to express my appreciation to Professor Ph.D. Paulo Cezar Leone for his valuable and constructive suggestions during the planning and development of this present paper. His willingness to give his time and effort so generously has been very much appreciated.

I would also like to thank the company *Hydrel HidroEletricidade Ltda* for enabling me to present this work.

## 9. REFERENCES

- Abbott, I. H., 1958. *Theory of Wing Sections*. New York: Dover Publications.
- Breslin, J. P., 1961. *A Manual For Calculation Of Inception of Cavitation on Two And Three Dimensional Forms*. New York: The Society of Naval Architects and Marine Engineers.
- Carpenter, H., 2003. *Aerodynamics for Engineering Students*. Oxford: Butterworth-Heinemann.
- Ghose, J., 2004. *Basic Ship Propulsion*. New Delhi: Allied Publishers.
- Gostelow, J., 1984. *Cascade Aerodynamics*. Sydney, Australia: Pergamon Press.
- IEC 60041., 1991. "Field Acceptance Tests to Determine the Hydraulic Performance of Hydraulic Turbines, Storage Pumps, and Pump-Turbines", 3<sup>rd</sup> edition.
- Kruppa, C. F., 1969. *High Speed Propellers Hydrodynamics and Design*. Michigan: The University of Michigan.
- Lewis, R., 1991. *Vortex Element Methods for Fluid Dynamic Analysis of Engineering Systems*. New York: Cambridge.
- NBR11374, A., 1990. *Turbinas hidráulicas - Ensaio de campo*. Rio de Janeiro: ABNT.
- Twhaites, B., 1987. *Incompressible aerodynamics*. Oxford: Dover.

## 10. RESPONSIBILITY NOTICE

The authors are the only responsible for the printed material included in this paper.